NASA TM-81842

NASA Technical Memorandum 81842

APPLICATION OF FULLY STRESSED DESIGN PROCEDURES TO REDUNDANT AND NON-ISOTROPIC STRUCTURES

Howard M. Adelman, Raphael T. Haftka and Uri Tsach

July 1980

NASA

National Aeronautics and
Space Administration

Langley Research Center
Hampton, Virginia 23665

SUMMARY

This paper discusses an evaluation of fully stressed design procedures for sizing highly redundant structures including structures made of composite materials. The evaluation is carried out by sizing three structures: a simple box beam of either composite or metal construction; a low aspect ratio titanium wing; and a titanium arrow wing for a conceptual supersonic cruise aircraft. All three structures are sized by ordinary fully-stressed design (FSD) and thermal fully stressed design (TFSD) for combined mechanical and thermal loads. Where possible, designs are checked by applying rigorous mathematical programing techniques to the structures. It is found that FSD and TFSD produce optimum designs for the metal box beam, but produce highly non-optimum designs for the composite box beam. Results from the delta wing and arrow wing indicate that FSD and TFSD exhibit slow convergence for highly redundant metal structures. Further, TFSD exhibits slow oscillatory convergence behavior for the arrow wing for very high temperatures. In all cases where FSD and TFSD perform poorly either in obtaining non-optimum designs or in converging slowly, the assumptions on which the algorithms are based are grossly violated. The use of scaling, however, is found to be very effective in obtaining fast convergence and efficiently produces safe designs even for those cases when FSD and TFSD alone are ineffective.

INTRODUCTION

Probably the most widely-used approach for sizing of flight structures subjected to strength and minimum gage constraints is fully stressed design (FSD). In this method, structural element resizing is based on the ratio of calculated stress to allowable stress. The FSD procedure traditionally is used to obtain, at reasonable computational cost, designs which, if not at minimum mass, are at least acceptably close to minimum mass (refs. 1-5). Recently, thermal stresses have been accounted for in a variant of FSD denoted TFSD (thermal fully stressed design) which overcomes many of the shortcomings of FSD when thermal stresses are comparable in magnitude to the mechanical stresses (refs. 6-8).

The FSD and TFSD procedures have been established for a variety of structural finite elements and have been incorporated into general-purpose structural sizing computer programs (refs. 9-11). Additionally, the success of FSD has aided the development of optimality criterion techniques in that some recursive formulas used in that more rigorous approach are based on FSD (ref. 12). Most of the use of FSD and TFSD has been for moderately redundant metal structures. There is a temptation to apply these methods to a more general class of structures. It has been shown for simple examples, however, that FSD can produce highly non-optimum designs for structures composed of several different materials or structures having a high degree of redundancy (ref 13).

The objective of the present paper is to further assess the appropriateness of FSD procedures through studies of redundant wing structures composed of isotropic and non-isotropic (i.e., composite) materials. Three finite element modeled structures are used to perform the evaluation: a rectangular box beam of either aluminum or graphite/polyimide construction, a low-aspect-ratio titanium delta wing and a titanium arrow wing for a conceptual supersonic cruise aircraft (SCR). The model for the delta wing is coarse and is intended as a demonstration of the methodology. The model for the arrow wing is more refined and is intended for use in preliminary design studies. Final designs obtained by FSD for the first two structures are checked by applying rigorous mathematical programing techniques to the structures. For all three examples, performance of FSD and TFSD is also evaluated by studying the convergence behavior of the methods. As part of this evaluation, the usefulness of scaling combined with FSD is investigated especially for those cases where FSD and TFSD exhibit extremely slow convergence.

LIST OF SYMBOLS

A	= area of a bar element
b	= $2\sigma_{xT}\sigma_{xM} + 2\sigma_{yT}\sigma_{yM} - \sigma_{xT}\sigma_{yM} - \sigma_{yT}\sigma_{xM} + 6\sigma_{xyT}\sigma_{xyM}$ thermal-mechanical coupling term
E_1, E_2	= Young's modulus in fiber and transverse directions
F_1	= $1/X_T + 1/X_C$
F_2	= $1/Y_T + 1/Y_C$
F_{11}	= $-1/X_T X_C$
F_{22}	= $-1/Y_T Y_C$
F_{66}	= $1/S^2$
G	= shear modulus
N_x, N_y, N_{xy}	= forces per unit length
P	= pressure
S	= shear strength
T	= temperature
t	= membrane thickness
V	= $(\sigma_x^2 + \sigma_y^2 - \sigma_x\sigma_y + 3\sigma_{xy}^2)^{1/2}$, Von Mises stress
X_T, X_C	= tensile and compressive strengths in fiber direction

2

Y_T, Y_C	= tensile and compressive strengths in transverse direction
α_1, α_2	= coefficients of thermal expansion in fiber and transverse directions
$\sigma_x, \sigma_y, \sigma_{xy}$	= stress components
σ	= uniaxial stress

Subscripts

a	= allowable
i	= iteration number
M	= mechanical
T	= thermal

REVIEW OF FSD AND TFSD

In the method of fully stressed design (FSD) for uniaxial elements, the basis for structural resizing is the ratio of the total stress (mechanical plus thermal) to the allowable stress and is predicated on the assumption that the force in each member is constant during resizing. The FSD algorithm is given by

$$A_{i+1} = \frac{\sigma_{Mi} + \sigma_{Ti}}{\sigma_a} A_i \qquad (1)$$

In equation (1), σ_M is the stress due to mechanical loads acting alone, σ_T is the stress due to thermal loads acting alone, and σ_a is either the tensile or compressive allowable stress, depending on the sign of the total stress as given by the numerator.

The basis for the thermal fully stressed design (TFSD) algorithm (ref. 6) is that during resizing the thermal stress and the mechanical force each remain constant. The TFSD resizing algorithm for uniaxial stress members from reference 7 is

$$A_{i+1} = \frac{\sigma_{Mi}}{\sigma_a - \sigma_{Ti}} A_i \qquad (2)$$

3

where σ_a is either the tensile or compressive allowable stress, depending on the sign of σ_M. FSD and TFSD sizing formulas for isotropic, orthotropic and composite membrane elements have also been developed (see refs. 6-8) and are summarized in table 1. The fully-stressed conditions for isotropic and nonisotropic membranes are defined by the Von Mises and Tsai-Wu (ref. 14) failure theories, respectively.

An alternate and conservative approach sometimes used (e.g., ref. 15) in designing for combined thermal and mechanical stress is to sum thermal and mechanical stresses in a sizing formula only if these stresses have the same sign (i.e. compensating effects are neglected). This approach has not been implemented in the present work.

THE PARS PROGRAM

PARS (Program for Analysis and Resizing of Structures, ref. 16) was developed for obtaining minimum mass designs of structures modeled by finite elements. It can be used for flutter analysis, calculation of derivatives of stress, displacements, and flutter speeds with respect to structural parameters, and for resizing structures subject to stress, displacement and flutter constraints. PARS has both a mathematical programing algorithm based on an extended interior penalty function approach (ref. 17) and FSD/TFSD algorithms. PARS uses the SPAR (ref. 18) finite element structural analysis program and like SPAR, it is composed of a number of individual processors that communicate through a data base. The individual processors can be called in sequence by the user to perform analysis, sensitivity and resizing operations. Automatic looping procedures are also available which enable the user to direct PARS to perform a specified number of resizing operations. In the application to the delta wing and the arrow wing, the automatic looping system was used for 10-25 iterations at a time.

EVALUATION OF FSD AND TFSD FOR BOX BEAM

The applicability of FSD and TFSD to composite structures is investigated by calculations for the box beam shown in figure 1 and described in detail in references 8 and 19. Calculations are carried out for a graphite/polyimide box beam, and for reference purposes for an aluminum box beam, using a computer program incorporating the FSD and TFSD algorithms as well as mathematical programing techniques using the AESOP optimization program (ref. 20). Finite-element methods using standard rod elements and the "TRIM 6" (ref. 21) triangular membrane elements were used for the analysis, with the upper and lower covers modeled with membranes and the interior structure modeled with trusses to represent shear panels. The box beam is built-in at the root. The loads consist of in-plane forces, normal pressure applied to the upper and lower covers, as well as applied temperatures.* The aluminum box beam is designed for the case of a temperature gradient through the depth of the

_____

*Plate bending and buckling due to pressure loads are both neglected in the analysis

4

structure, while the graphite polyimide box beam is designed for both a uniform temperature and a temperature gradient through the depth. The loads are summarized in Table 2, and the material properties are given in Table 3. The bars in the graphite/polyimide box beam are assigned uniaxial properties corresponding to the fiber direction of the composite (i.e. $E = E_1$ and $a = X_T$ or X_c). The finite-element model of the structure consists of 68 bars, 8 membranes, and 30 grid points (fig. 2). A design variable is assigned to each membrane thickness and rod cross sectional area. In the composite model, each ply is modeled by a separate membrane element. The following minimum gage values were used: for the aluminum wing box-thickness 0.06cm (0.025 in.) and rod cross sectional areas 1.72cm^2 (0.267in^2); for the composite wing box the thickness 0.0076cm (0.003 in.) and rod cross sectional area 1.03 cm^2 (0.160 in.^{2}).

Convergence of FSD and TFSD for the aluminum box beam is shown in figure 3. Both FSD and TFSD converge rapidly as might be expected with TFSD converging faster than FSD primarily due to the faster convergence of the membrane elements which have large thermal stresses. Convergence behavior for the graphite polyimide box beam with uniform and nonuniform temperature is shown in figures 4 and 5 respectively. Both FSD and TFSD converge much more slowly for the composite material than for the metal, due to the high redundancy of the composite skin. The final design for the non uniform temperature case (fig. 5) has less mass than the design for uniform temperature (fig. 4). This result is attributed to the fact that the low temperature on the top surface is associated with higher allowable stresses.

The optimality of the final designs produced by FSD and TFSD is evaluated by comparisons with designs from a mathematical programing approach (ref. 20). To keep the mathematical programing problem to a manageable size, comparisons are based on designs where only the skin (membrane) elements are sized. The comparisons are given in Tables 4, 5 and 6. As indicated in Table 4, designs for the aluminum box beam by FSD, TFSD and mathematical programing are identical. For the composite box beam (Tables 5 and 6), FSD and TFSD obtained the same design but the designs were different from the designs from mathematical programing (about 12 percent heavier for the uniform temperature case and about 6 percent heavier for the non-uniform temperature case). Typically, the converged mathematical programing designs were obtained after 60-80 resizing steps.

The non-optimality of the composite box beam designs, especially for the uniform temperature case, prompted a further study of this structure--namely to determine the effect of the magnitude of temperature loading on the optimality of FSD-produced designs. In this study, comparisons between designs from FSD and mathematical programing were made for uniform temperature rises ranging between OK and 167K (0°F and 300°F). Results of this study are presented in Table 7 and figure 6 and indicate that FSD and TFSD produced extremely non optimum designs for small thermal loads. In these cases, when FSD was started close to the optimum design the optimum final design was obtained. An explanation offered for this behavior is that for low temperatures there is more than one fully stressed design. One of these (obtained by mathematical programing) is optimum and the other (which is much different from the first)

is reached by FSD when started at an arbitrary initial design. Further, the FSD design is not even a local minimum since the mathematical programing procedure did not produce this design when started close to it. For higher temperatures, the fully stressed designs are assumed to coalesce since FSD obtains the optimum design.

It is noted from Tables 5 and 6 that there are large differences in thicknesses of adjacent elements in the composite designs. These are, in part, due to the coarse model used in the calculations. Nontheless, it is expected that the trends shown in Table 7 and figure 6 remain valid for more refined models.

EVALUATION OF FSD AND TFSD FOR DELTA WING

A titanium delta wing was chosen as an example of a low aspect ratio wing structure to further evaluate FSD and TFSD for redundant metal structures. A SPAR finite element model of the wing (shown in figure 7) includes 51 membranes, 49 shear panels, 31 rod elements, and 76 grid points. The following minimum gages were used: membrane thickness 0.051 cm (0.02 in.), shear panel thickness 0.0762cm (0.03 in.), and rod areas 0.645cm^2 (0.10 in.^{2}). The model is shown in figure 7. Due to symmetry only the upper half of the wing is modeled. Complete details of the finite element model are given in reference 22. The wing is subjected to an air load of 6895 N/M^2 (1.0 psi) and a set of applied temperatures given in Table 8. The designs by FSD, TFSD, and mathematical programing are obtained by use of the PARS computer program (ref. 10).

The first calculation deals with optimizing only the membrane elements of the wing while the remaining elements have fixed sizes. As a result there are 51 design variables in the problem. Convergence of FSD and TFSD is shown in figure 8. Both methods converge rapidly (FSD requires 4 iterations to converge to within 5 percent of the final mass and TFSD requires 2 iterations) and the final mass agrees closely with the mass obtained by the mathematical programing option in PARS. The mathematical programing design was obtained in 20 iterations.

To bring out the effect of redundancy on the performance of FSD, the same wing was designed with all elements being sized (resulting in 131 design variables). Temperature loads were omitted. As shown in figure 9, convergence was much slower than in the previous case where only the skin was sized. Evidently, the high redundancy of the internal structure slows down the convergence of the FSD procedure. The type of slow convergence displayed in this example may often be alleviated by the use of scaling. In this approach after each FSD iteration all structural sizes are multiplied by the maximum stress ratio. Application of scaling to the present problem leads to the dashed curve in figure 9. Because each of the scaled designs has a maximum stress ratio of 1.0 it is possible to terminate the design process after a small number of iterations and obtain a safe design close to optimum mass with a reasonable computational effort. In this example, only five iterations are required to obtain a design having a mass within three percent of the converged

6

design. At this same iteration, FSD without scaling produces a design which is within five percent of the final mass but has elements which are overstressed by about eight percent. Additional illustrations of scaling are included in the next example.

EVALUATION OF FSD AND TFSD FOR SCR WING

Model Definition and Loads

An arrow wing for a conceptual supersonic cruise aircraft (SCR) was used as an example of a complex highly-redundant metal structure. The SPAR finite element model of the titanium structure (described in detail in ref. 23) is shown in figure 10. The model is composed of quadrilateral and triangular membrane elements for the skin, with shear panels and rod elements for the internal structure. The model has 753 grid points and 2369 elements. There are 334 design variables assigned to the membrane element thicknesses, 384 design variables assigned to the shear panel thicknesses and 25 design variables assigned to the rod cross-sectional areas. Minimum gages were as follows: membrane thicknesses 0.0762cm (0.03 in), shear panel thicknesses 0.032 cm (0.0124 in.), and rod areas 0.645 cm^2 (0.10 in.^{2}). The finite elements used to model the fuselage are not sized. Five load cases summarized in Table 9 are considered. In the first four cases the mechanical loads are augmented by temperatures (from ref. 24) given in figure 11.

Results and Discussion

The arrow wing model was sized for mechanical and thermal loads using the FSD and TFSD procedures in PARS. Additionally, the wing with only mechanical loads was sized by FSD. Results are shown in figure 12. The slow convergence of FSD and TFSD exhibited in the delta wing example is even more evident in this example. Because of the cost of the analysis (about 570 CPU sec* per iteration) the process was terminated after 25 iterations. At the 25th iteration, the mass was still increasing and the maximum stress ratio was about 1.05. Thermal stresses in this problem were small and had little effect on the design process as evidenced by the closeness of the curves for FSD with and without temperature loads. Consistently, there was little difference in the convergence behavior of FSD and TFSD. As was the case for the delta wing, scaling provides a way of terminating the design process after a few iterations while providing a reasonable design. In this example, six scaling iterations give a design having a mass within three percent of the mass at iteration 25.

A second set of design calculations was carried out for the arrow wing to determine the effects of extremely high thermal stresses on the performance of FSD and TFSD for a highly redundant problem. In this example, the temperatures at points on the wing in the vicinity of the engines were prescribed to have (admittedly unrealistically high) temperatures of 811K (1000°F), while the

---

*Time is for the Langley Research Center Cyber 173 computer using the NOS 1.2 operating system.

remaining temperatures and mechanical loads were unchanged. Results of the calculations are shown in figure 13. The behavior of FSD is not significantly affected by the higher temperatures. The TFSD behavior is drastically affected as it experiences large oscillations in mass which are damped very slowly. The oscillations result from the simultaneous occurance of several conditions in certain critical shear panel elements: (1) the thermal stresses are close to or exceed the allowable stresses; (2) the thermal and mechanical stresses have opposite signs; (3) the structure is highly redundant. With reference to figure 13 and equation (2), the iteration history begins with a minimum gage structure in which both the mechanical and thermal stresses are large. During iterations 1-5 the structural elements are increased in size until at iteration 5 the mechanical stresses are reduced substantially and excessively. At iteration 5, some thermal stresses exceed the allowable stresses and the compensating mechanical stresses are so small that the total stress exceeds the allowable stress. Thus, TFSD increases the compensating mechanical stress by large decreases in structural sizes in iterations 6 and 7. At iteration 7 the mechanical stresses are again too large and structural size increases are called for. Ordinarily this pattern of osciallation (if it occurred at all) would be quickly damped and the procedure would converge. In the present case damping is slow because of the unusual conditions cited previously and the oscillations continue with low damping.

Finally, FSD with scaling is found to be effective for this problem as indicated by the dashed-dot curve in figure 13. After nine iterations of FSD with scaling, a feasible design is produced which has 3 percent more mass than the design at the 25th iteration (where the design appears to be essentially converged). Using FSD without scaling, the design, after nine iterations, has a mass which is 7 percent higher than the mass at iteration 25 and has elements overstressed by over 18 percent.

It is concluded from the examples herein that FSD and TFSD may display poor performance when applied to structures having high redundancy, composite materials and excessively high thermal stresses. This result should not be surprising since FSD and TFSD are based on assumptions which exclude the conditions cited. The use of an appropriate scaling strategy, however, can be used to extend the applicability of FSD and TFSD to structures for which FSD and TFSD are otherwise inapplicable.

CONCLUDING REMARKS

This paper discusses application of fully stressed design procedures to redundant structures and structures composed of nonisotropic materials including composites. Evaluations are carried out by applications to sizing three structures: a simple box beam with either composite or metal construction; a low aspect ratio titanium delta wing; and titanium arrow wing for a conceptual supersonic cruise aircraft. All three structures are sized by ordinary fully-stressed design (FSD) and thermal fully stressed design (TFSD) for combined mechanical and thermal loads. Where possible (for the box beam and the delta wing), designs are checked by applying mathematical programing techniques to the structures.

It is found from the box beam examples that use of FSD and TFSD for a composite structure may yield highly non-optimum designs. Conversely, for the metal box beam, FSD and TFSD computed designs are very close to optimum. It is suggested that the poor performance for the composite case stems from the redundancy and anisotropy of the composite construction.

Results from the delta wing example indicate that FSD and TFSD exhibit slow convergence for highly redundant metal structures. Specifically, for the less redundant case when only the skin elements of the wing are sized, convergence to within 3 percent of the final mass is achieved in 2 TFSD steps and 4 FSD steps and close agreement with the optimum design from mathematical programing is obtained. When the entire wing including the internal structure is sized, twenty-five iterations are required for convergence. On the positive side, the use of scaling is very effective in improving convergence of the delta wing design (five iterations produce a design having only 3 percent more mass than the converged design).

Results from the arrow wing example again demonstrate the slow convergence of FSD and TFSD for a highly redundant metal structure. Both procedures are terminated (due to cost considerations) after 25 iterations while far from convergence. Scaling again is quite useful - in only 6 iterations producing a design in which all stresses are acceptable and the mass is the same as that at iteration 25 without scaling. When the arrow wing is sized for the case of excessively high temperatures at certain points on the structure, erratic convergence of TFSD is observed. This is due to the presence of extremely large thermal stresses and the high redundancy of the structure. Stress ratio scaling is found to alleviate the poor convergence even for this high temperature case.

In all cases where FSD and TFSD perform poorly either in obtaining non-optimum designs or in converging slowly, the assumptions on which the algorithms are based are grossly violated. The above findings would indicate that judgement should be used in the application of these techniques to highly redundant and/or anisotropic structures particularly fiber reinforced composites. The results also indicate that scaling is a useful technique which is often able to produce satisfactory designs even for the most challenging situations.

9

REFERENCES

1. Gellatly, R. A.; Gallagher, R. H.; and Luberacki, W. A.: Development of a Procedure for Automated Synthesis of Minimum Weight Structures. FDL-TDR-64-141, U. S. Air Force, Oct. 1964. (Available from DDC as AD 611 310).

2. Razani, Reza: Behavior of Fully Stressed Design of Structures and its Relationship to Minimum Weight Design. AIAA Journal, Vol. 3, No. 12, Dec. 1965, pp 2262-2268.

3. Dayaratram, P.; and Patnaik, S.: Feasibility of Full Stress Design. AIAA Journal, Vol. 7, No. 4, April 1969, pp 773-774.

4. Lansing, W.; Dwyer, W.; Emerton, R.; and Ranalli, E.: Application of Fully-Stressed Design Procedures to Wing and Empennage Structures. J. Aircraft, Vol. 8, No. 9, Sept. 1971, pp. 683-688.

5. Giles, Gary L.; Blackburn, Charles L.; and Dixon, Sidney C.: Automated Procedures for Sizing Aerospace Vehicle Structures (SAVES). J. Aircraft, Vol. 9, No. 12, Dec. 1972, pp. 812-819.

6. Adelman, Howard M.; Walsh, Joanne L.; and Narayanaswami, R.: An Improved Method for Optimum Design of Mechanically and Thermally Loaded Structures. NASA TN D-7965, 1975.

7. Adelman, H. M. and Narayanaswami, R.: Resizing Procedure for Structures under Combined Mechanical and Thermal Loading. AIAA Journal, Vol. 14, Oct. 1976, pp. 1484-1486.

8. Adelman, Howard M.; Sawyer, Patricia L.; and Shore, Charles P.: Optimum Design of Structures at Elevated Temperatures. AIAA Journal, Vol. 17, No. 6, June 1979, pp. 622-629.

9. Driesback, R. L.: ATLAS - An Integrated Structural Analysis and Design System - ATLAS User Guide. NASA CR-159041, 1979.

10. Haftka, R. T.; Prasad, B.; and Tsach, U.: PARS--Programs for Analysis and Resizing of Structures--User Manual. NASA CR-159007, 1979.

11. Kiusalaas, J.; and Reddy, G. B.: DESAP 2--A Structural Design Program with Stress and Buckling Constraints. NASA CR-2797, March 1977.

12. Venkayya, V. B.; Khot, N. S.; and Berke, L.: Application of Optimality Criteria Approaches to Automated Design of Practical Structures. AGARD-AP-123, pp. 3-1-3-19, 1973.

13. Pope, G. G.; and Schmit, L. A.: Structural Design Applications of Mathematical Programing Technique. AGARD-ograph-149, Feb. 1971.

10

14. Tsai, S. W.; and Wu, E. M.: A General Theory of Strength for Anisotropic Materials. J. Comp. Mat'l, Vol. 5, Jan. 1971, pp. 58-80.

15. Deriugin, V.; Brogren, E. W.; Jaeck, C. L.; Brown, A. L.; and Clingan, B. E.: Thermal Structural-Combined Loads Design Criteria Study. NASA CR-2102, 1972.

16. Haftka, R. T.; and Prasad B.: Programs for Analysis and Resizing of Complex Structures. Computers and Structures, Vol. 10, pp. 323-330, 1979.

17. Haftka, R. T.; and Starnes, J. H., Jr.: Applications of a Quadratic Extended Interior Penalty Function for Structural Optimization. AIAA J. Vol. 14, pp. 718-724, 1976.

18. Whetstone, W. D.: SPAR Structural Analysis System, Reference Manual. NASA CR-158970, 1978.

19. Adelman, H. M.; and Sawyer, P. L.: Inclusion of Explicit Thermal Requirements in the Optimum Design of Structures. NASA TM X-74017, 1977.

20. Jones, R. T.; and Hague, D. S.: Application of Multivariable Search Techniques to Structural Design Optimization. NASA CR-2038, 1972.

21. Argyris, J. H.: Triangular Elements with Linearly Varying Strain for the Matrix Displacement Method Journal of the Royal Aeronautical Society, Vol. 69, Oct. 1965, pp 711-713.

22. Haftka, R. T.; and Starnes, J.H., Jr.: WIDOWAC (Wing Design Optimization with Aeroelastic Constraints): Program Manual. NASA TM X-3071, Oct. 1974.

23. Sobieszczanski, J.; McCullers, L. A.; Rickets, R. H.; Santoro, N. J.; Beskenis, S. D.; and Kurtze, W. L.: Structural Design Studies of Supersonic Cruise Aircraft Wing Configuration. NASA CP-001, Nov. 1976, pp. 659-684.

24. Wright, B. R.; Sedgwick, T. A.; and Urie, D. M.: An Advanced Concept that Promises Ecological and Economic Viability. NASA CP-001, Nov. 1976, pp. 938-984.

TABLE 1. – FSD and TFSD Algorithms For Various Structural Elements

Element Type	FSD	TFSD
Bar	$\dfrac{A_{i+1}}{A_i} = \dfrac{\sigma_M + \sigma_T}{\sigma_a}$	$\dfrac{A_{i+1}}{A_i} = \dfrac{\sigma_M}{\sigma_a - \sigma_T}$
Isotropic Membrane	$\dfrac{t_{i+1}}{t_i} = \dfrac{V_i}{\sigma_a}$	$\dfrac{t_{i+1}}{t_i} = \dfrac{b}{2(\sigma_a^2 - \sigma_T^2)} + \left[\dfrac{b^2}{4(\sigma_a^2 - V_T^2)^2} + \dfrac{V_M^2}{\sigma_a^2 - V_T^2} \right]^{1/2}$
Composite Lamina or Orthotropic Membrane	$\dfrac{t_{i+1}}{t_i} = \dfrac{B}{2}\left[+ \left(\dfrac{B}{2}\right)^2 + C \right]^{1/2}$	$\dfrac{t_{i+1}}{t_i} = \dfrac{B_m + D_{mT}}{2(1-F_T)} +$ $+ \left[\left(\dfrac{B_m + D_{mT}}{2(1-F_T)}\right)^2 + \dfrac{C_m}{1-F_T} \right]^{1/2}$

$$V = \left[\sigma_1^2 + \sigma_2^2 - \sigma_1\sigma_2 + 3\sigma_{12}^2 \right]^{1/2}$$

$$b = 2\sigma_{1T}\sigma_{1M} + 2\sigma_{2T}\sigma_{2M} - \sigma_{1T}\sigma_{2M}$$
$$- \sigma_{1M}\sigma_{2T} + 6\sigma_{12T}\sigma_{12M}$$

$$F = B + C$$

$$B = F_1\sigma_1 + F_2\sigma_2$$

$$C = F_{11}\sigma_1^2 + F_{22}\sigma_2^2 + F_{66}\sigma_{12}^2$$

$$D_{mT} = 2F_{11}\sigma_{1M}\sigma_{1T} + 2F_{22}\sigma_{2M}\sigma_{2T}$$
$$+ 2F_{66}\sigma_{12M}\sigma_{12T}$$

$$F_1 = 1/X_T + 1/X_c$$

$$F_2 = 1/Y_T + 1/Y_c$$

$$F_{11} = -1/X_T X_c$$

$$F_{22} = -1/Y_T Y_c$$

$$F_{66} = 1/S^2$$

$$F_{12} = \begin{cases} 0 \text{ for composite} \\ F_{11} \text{ otherwise} \end{cases}$$

TABLE 2. - Mechanical and Thermal Loads on Box Beam

(a) Mechanical Loads

		Upper Surface	Lower Surface
N_x	kN/m	-58.8	- 700
	lbf/in	-336	-4000
N_y	kN/m	-210	228
	lbf/in	-1200	1300
N_{xy}	kN/m	92	22.4
	lbf/in	528	128
P	Pa	276	6895
	psi	.04	1.0

(b) Temperatures

Description		ΔT_{upper}	ΔT_{lower}
Aluminum with Temperature Gradient	K °F	61 110	153 275
Graphite/Polyimide Uniform Temperature	K °F	111 200	111 200
Graphite/Polyimide Temperature Gradient	K °F	- 56 -100	111 200

13

Table 3. - Material Properties Used in Box Beam Analysis

	Graphite/polyimide		Aluminum	
Property	RT	533K(500°F)	RT	450K(350°F)
E_1 GPa	133	133	73.0	69.6
psi	19.3×10^6	19.3×10^6	10.6×10^6	10.1×10^6
E_2 GPa	9.10	4.14	...	...
psi	1.32×10^6	0.6×10^6		
ν_{12}	0.37	0.51	0.33	0.33
G_{12} GPa	5.58	4.41		
psi	0.81×10^6	0.64×10^6	...	...
α_1 K^{-1}	-0.63×10^{-6}	0.144×10^{-6}	22.77×10^{-6}	24.8×10^{-6}
$°F^{-1}$	-0.38×10^{-6}	0.08×10^{-6}	12.65×10^{-6}	13.8×10^{-6}
α_2 K^{-1}	27.0×10^{-6}	45.0×10^{-6}		
$°F^{-1}$	15.0×10^{-6}	25.0×10^{-6}	...	...
X_T GPa	1.08	1.02	0.400	0.320
psi	157,400	147,300	58,000	46,400
X_C MPa	-867	-450	-400.	-300.
psi	-125,800	-65,200	-58,000	-43,500
Y_T MPa	16.5	6.62		
psi	2390	960	...	...
Y_C MPa	-109	-87.8		
psi	-15,790	-12,730	...	...
S MPa	93.8	53.1		
psi	13,600	7700	...	...
ρ kg/m³	1550		2800	
lbm/in.³	0.056		0.101	

Table 4. - Final Design* of Aluminum Box Beam Skin for $\Delta T)_{upper}$ = 61K (110°F), $\Delta T)_{lower}$ = 153K (275°F).

Element Number	Thickness		Element Number	Thickness	
	cm	in		cm	in
1	0.0635	0.025	5	0.2116	0.0833
2	0.0635	0.025	6	0.2520	0.0992
3	0.0635	0.025	7	0.2332	0.0918
4	0.0635	0.025	8	0.2360	0.0929

Total Mass = 105 kg (232 lbm)

*FSD, TFSD and Math Programing Produce Identical Designs

15

Table 5. – Comparison of FSD/TFSD and Math Programing Results for Graphite/Polyimide Box Beam Skin With ΔT = 111K (200°F)

	Ply Thickness for Triangle –							
	1		2		3		4	
Ply Angle	FSD/ TFSD	Math Program	FSD/ TFSD	Math Program	FSD/ TFSD	Math Program	FSD/ TFSD	Math Program
0°	.0076 .003	.0076 .003	.0076 .003	.0076 .003	.0076 .003	.0076 .003	.0076 .003	.0076 .003
45°	.0076 .003	.0076 .003	.0076 .003	.0076 .003	.0076 .003	.0097 .0038	.0076 .003	.0076 .003
-45°	.0127 .0050	.0137 .0054	.0142 .0056	.0152 .0060	.0157 .0062	.0150 .0059	.0140 .0055	.0147 .0058
90°	.0076 .003	.0076 .003	.0076 .003	.0076 .003	.0076 .003	.0076 .003	.0076 .003	.0076 .003

	5		6		7		8	
Ply Angle	FSD/ TFSD	Math Program	FSD/ TFSD	Math Program	FSD/ TFSD	Math Program	FSD/ TFSD	Math Program
0°	.0754 .0297	.0709 .0279	.7021 .2764	.5410 .2130	.1311 .0516	.1219 .0476	.2916 .1148	.2500 .0984
45°	.0076 .003	.0079 .0031	.0076 .003	.0109 .0043	.0076 .003	.0086 .0034	.0076 .003	.0945 .0372
-45°	.0076 .003	.0102 .0040	.0076 .003	.0076 .003	.0076 .003	.0076 .003	.0076 .003	.0076 .003
90°	.0076 .003	.0076 .003	.0076 .003	.0102 .0040	.0076 .003	.0079 .0031	.0076 .003	.0079 .0031

Top Entry (cm.)
Lower Entry (in.)

FSD/TFSD   Mass = 59 kg (129 lbm)

Math Programing Mass = 52 kg (115 lbm)

16

Table 6. - Comparison of FSD/TFSD and Math Programing Results for Graphite/Polyimide Box Beam Skin T_{upper} = -55K (-100°F), T_{lower} = 111K (200°F)

	Ply Thickness for Triangle -							
	1		2		3		4	
Ply Angle	FSD/ TFSD	Math Program	FSD/ TFSD	Math Program	FSD/ TFSD	Math Program	FSD/ TFSD	Math Program
0°	.0076 .003	.0076 .003	.0076 .003	.0076 .003	.0076 .003	.0076 .003	.0076 .003	.0076 .003
45°	.0076 .003	.0076 .003	.0076 .003	.0084 .0033	.0076 .003	.0076 .003	.0076 .003	.0076 .003
-45°	.0209 .0082	.0211 .0083	.0241 .0095	.0236 .0093	.0340 .0134	.0323 .0127	.0193 .0076	.0213 .0084
90°	.0076 .003	.0076 .003	.0076 .003	.0076 .003	.0076 .003	.0076 .003	.0076 .003	.0076 .003

	5		6		7		8	
Ply Angle	FSD/ TFSD	Math Program	FSD/ TFSD	Math Program	FSD/ TFSD	Math Program	FSD/ TFSD	Math Program
0°	.0980 .0386	.0962 .0379	.4966 .1955	.4714 .1856	.1453 .0572	.1372 .0540	.2756 .1085	.1956 .0770
45°	.0076 .003	.0076 .003	.0076 .003	.0086 .0034	.0076 .003	.0076 .003	.0076 .003	.0096 .0038
-45°	.0076 .003	.0076 .003	.0076 .003	.0076 .003	.0076 .003	.0076 .003	.0076 .003	.0076 .003
90°	.0076 .003	.0076 .003	.0076 .003	.0076 .003	.0076 .003	.0076 .003	.0076 .003	.0096 .0038

Top Entry (cm.)
Lower Entry (in.)

FSD/TFSD Mass = 54 kg (119 lbm)

Math Programing Mass = 51 kg (112 lbm)

Table 7. - Effect of Uniform Applied Temperature on Comparison of Final
Mass From FSD and Math Programing for Graphite/Polyimide Box
Beam Skin.

Temperature, ΔT		Mass			
		FSD/TFSD		Math Programing	
K	°F	kg	lbm	kg	lbm
0	0	380	836	69	151
28	50	292	644	64	141
55	100	205	453	55	122
83	150	122	268	54.9	121
111	200	59	129	52	115
139	250	34	74	30.4	67
167	300	30	65	30	65

Table 8. - Delta Wing Temperatures

Point	T(K)	T(°F)	Point	T(K)	T(°F)
1	475	395	39	469	385
2	475	395	40	469	385
3	475	395	41	469	385
4	469	385	42	458	365
5	469	385	43	458	365
6	455	360	44	458	365
7	455	360	45	458	365
8	467	380	46	467	380
9	467	380	47	467	380
10	467	380	48	467	380
11	467	380	49	467	380
12	467	380	50	467	380
13	467	380	51	467	380
14	480	405	52	480	405
15	480	405	53	480	405
16	467	380	54	467	380
17	467	380	55	467	380
18	467	380	56	467	380
19	467	380	57	467	380
20	478	400	58	483	410
21	478	400	59	483	410
22	464	376	60	472	390
23	464	376	61	472	390
24	464	376	62	472	390
25	480	405	63	483	410
26	469	385	64	475	395
27	469	385	65	475	395
28	469	385	66	475	395
29	478	400	67	482	407
30	480	404	68	483	410
31	480	404	69	483	410
32	469	385	70	475	395
33	469	385	71	475	395
34	480	405	72	486	415
35	480	405	73	486	415
36	469	385	74	476	397
37	478	400	75	486	415
38	478	400	76	486	415

Table 9. - Definition of the Loading Cases for SCR Arrow Wing

Load Case	Load Factor (g)	Mach No.	Altitude m. (ft)	Gross Mass kg (1bm)	Fuel Mass kg (1bm)	Remarks
Cruise	1.0	2.7	18 288 (60 000)	313 626 (691 545)	127 212 (280 503)	
Maneuver I	2.5	1.2	10 668 (35 000)	340 823 (751 514)	154 410 (340 473)	Symmetric Pull-up
Taxi	-2.0	0	0	345 578 (762 000)	158 654 (349 833)	Support on the nose and main gear. no aerodynamic lift
Maneuver II	2.5	1.2	6553 (21,500)	218 287 (480 807)	31 163 (68640)	Low-mass maneuver
Maneuver III	1.0	0.24	45 (150)	218 287 (480 807)	31 163 (68640)	Landing approach

Loads on upper surface

N_x N_{xy} P N_{xy} N_x N_y

$[0/\pm45/90]$

90°

0°

$[0/\pm45/90]$

N_x N_{xy} N_{xy} N_x N_y P

Loads on lower surface
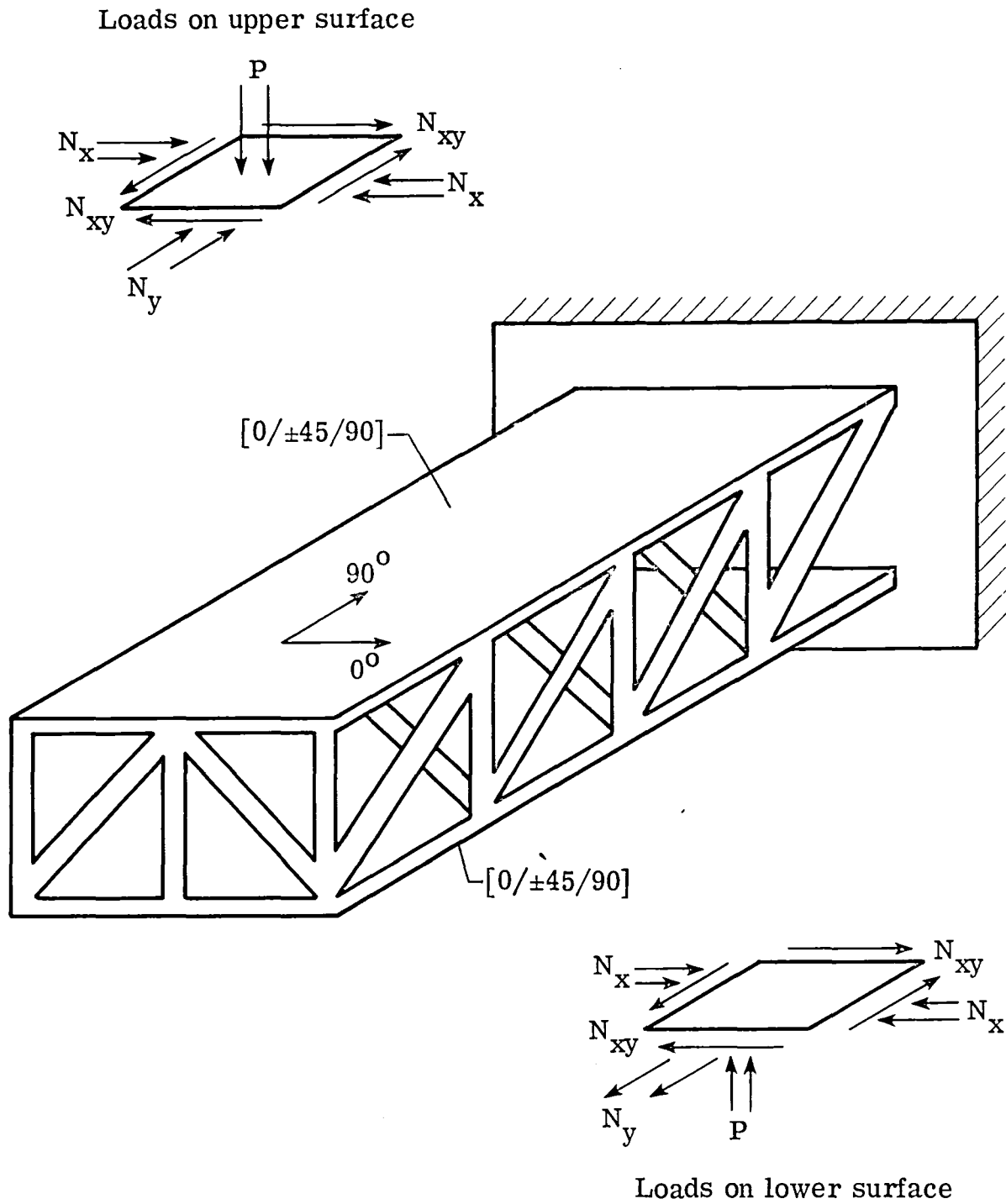
Figure 1.- Box beam model used to illustrate FSD and TFSD techniques.

21

(a) Covers
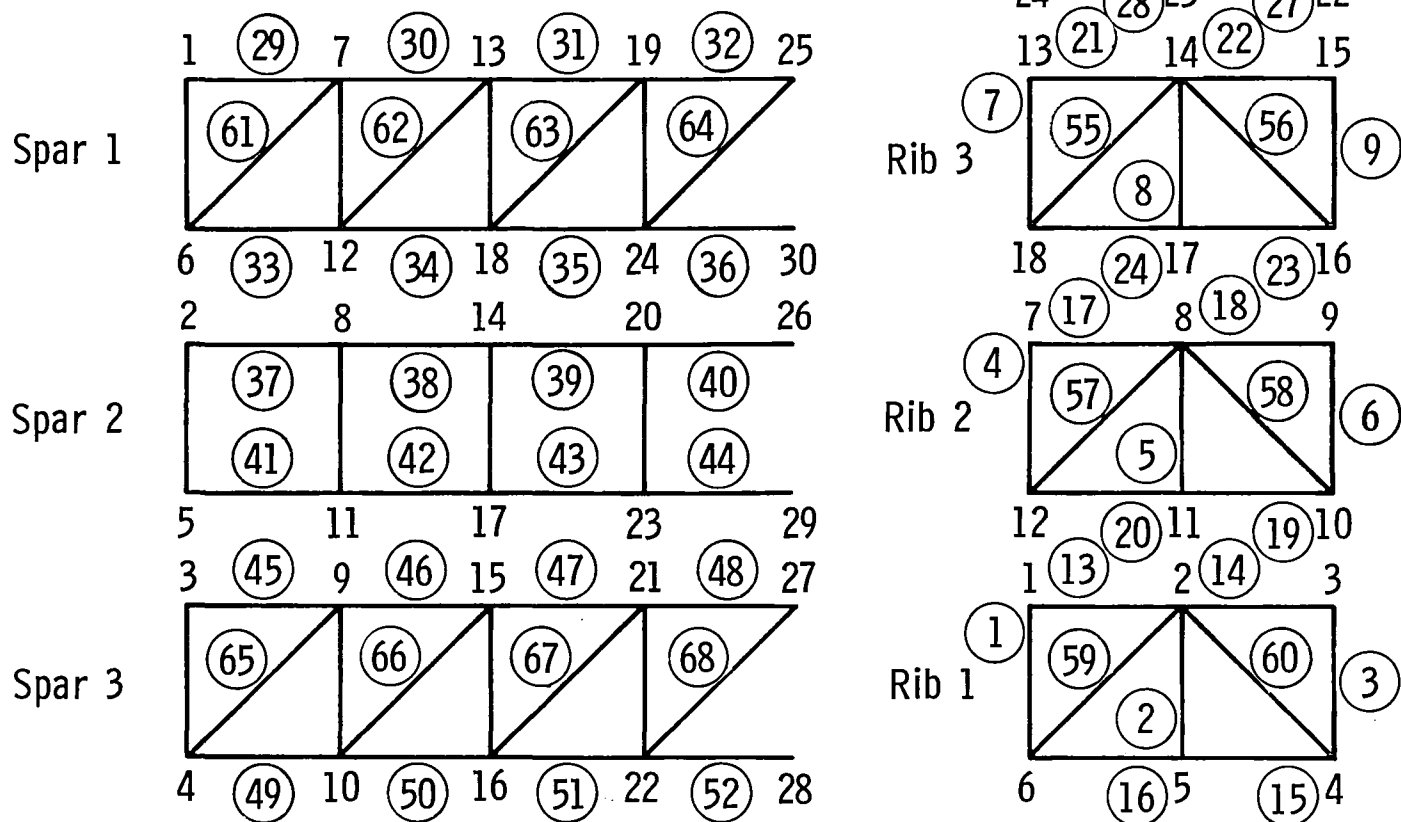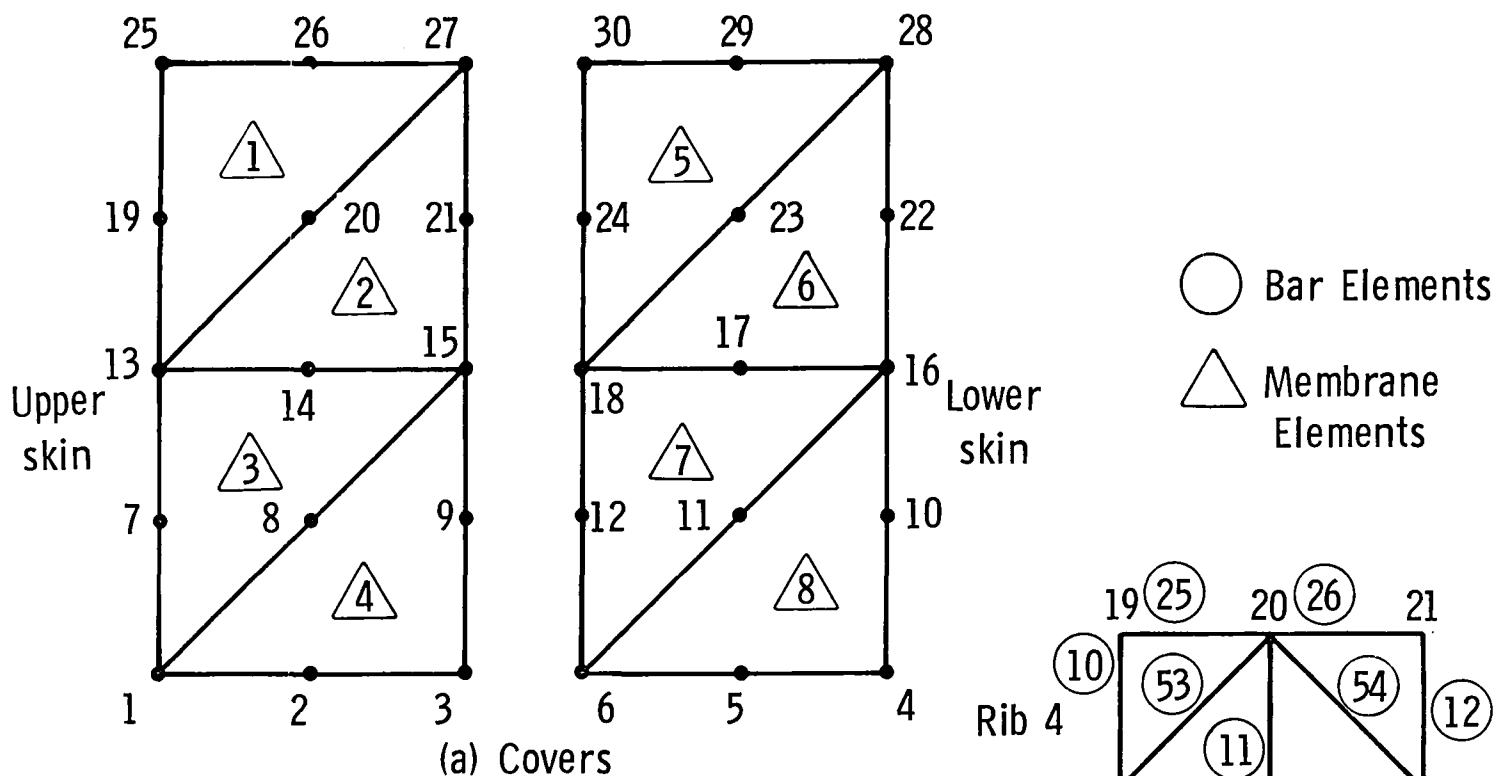
(b) Ribs and Spars

Figure 2. - Finite element model of box beam.
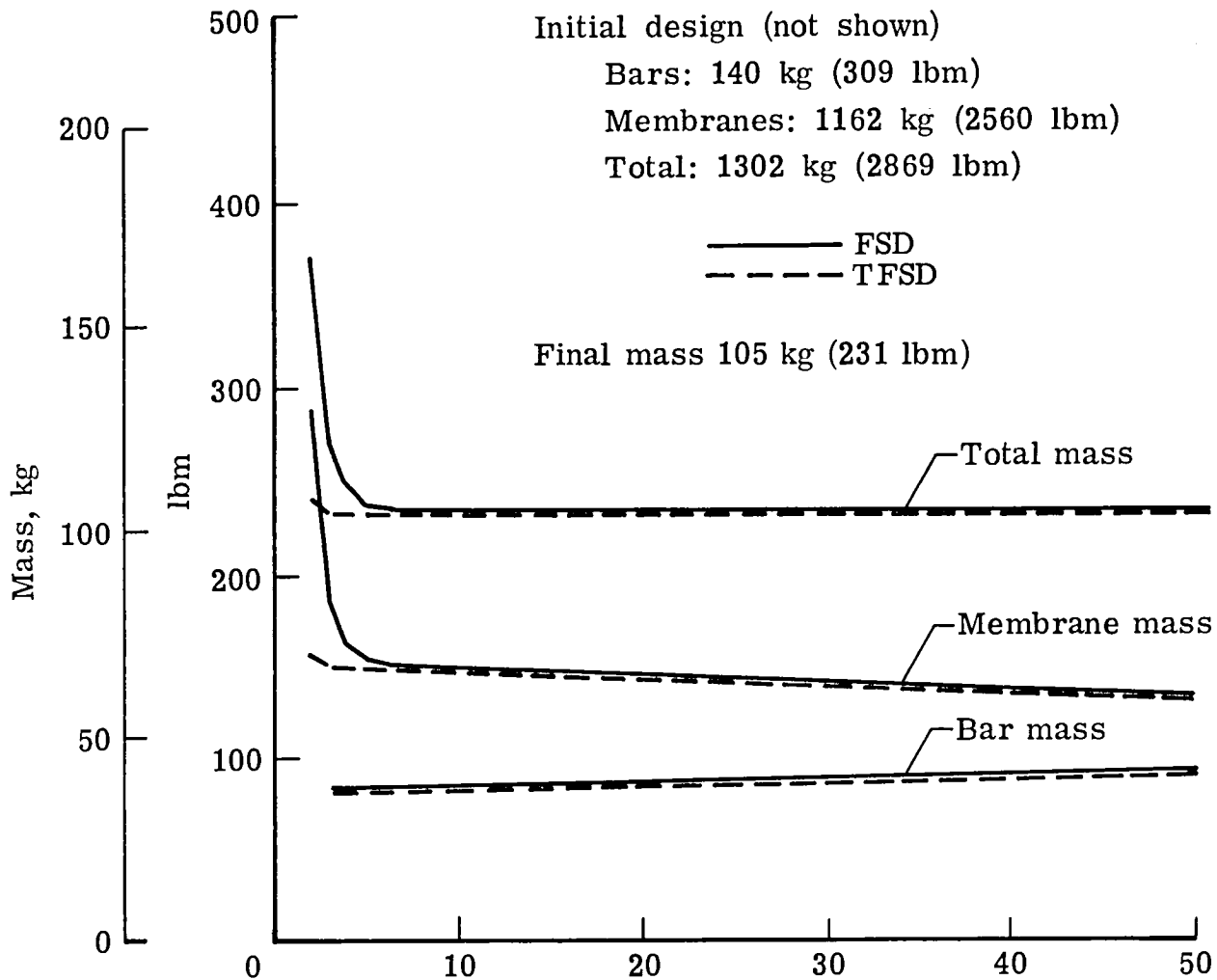
Figure 3.- Convergence of TFSD and FSD for aluminum box beam. $\Delta T_{upper} = 61$ K (110° F); $\Delta T_{lower} = 153$ K (275° F).
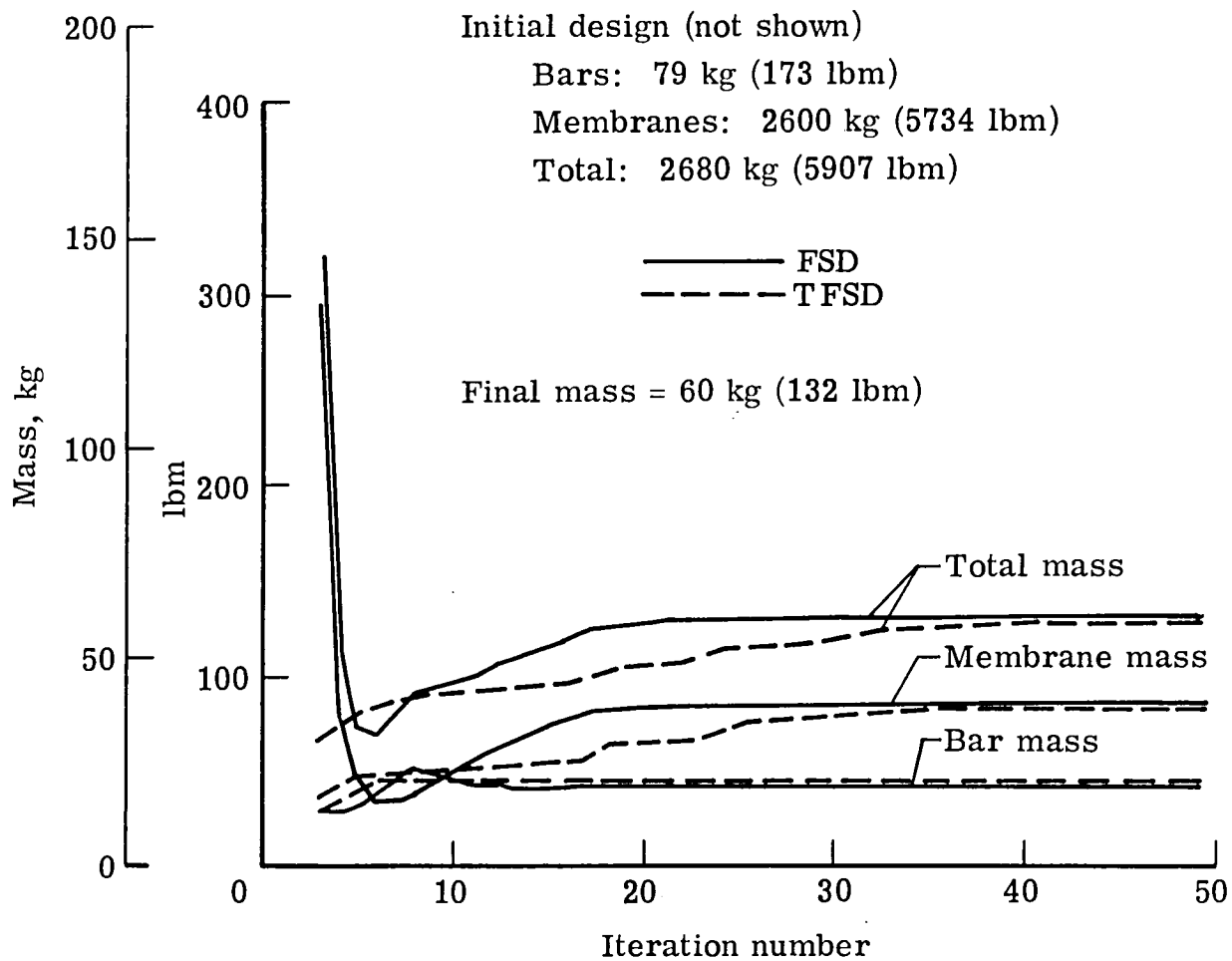
Figure 4.- Convergence of FSD and TFSD for graphite/polyimide box beam.
$\Delta T = 111$ K (200° F).
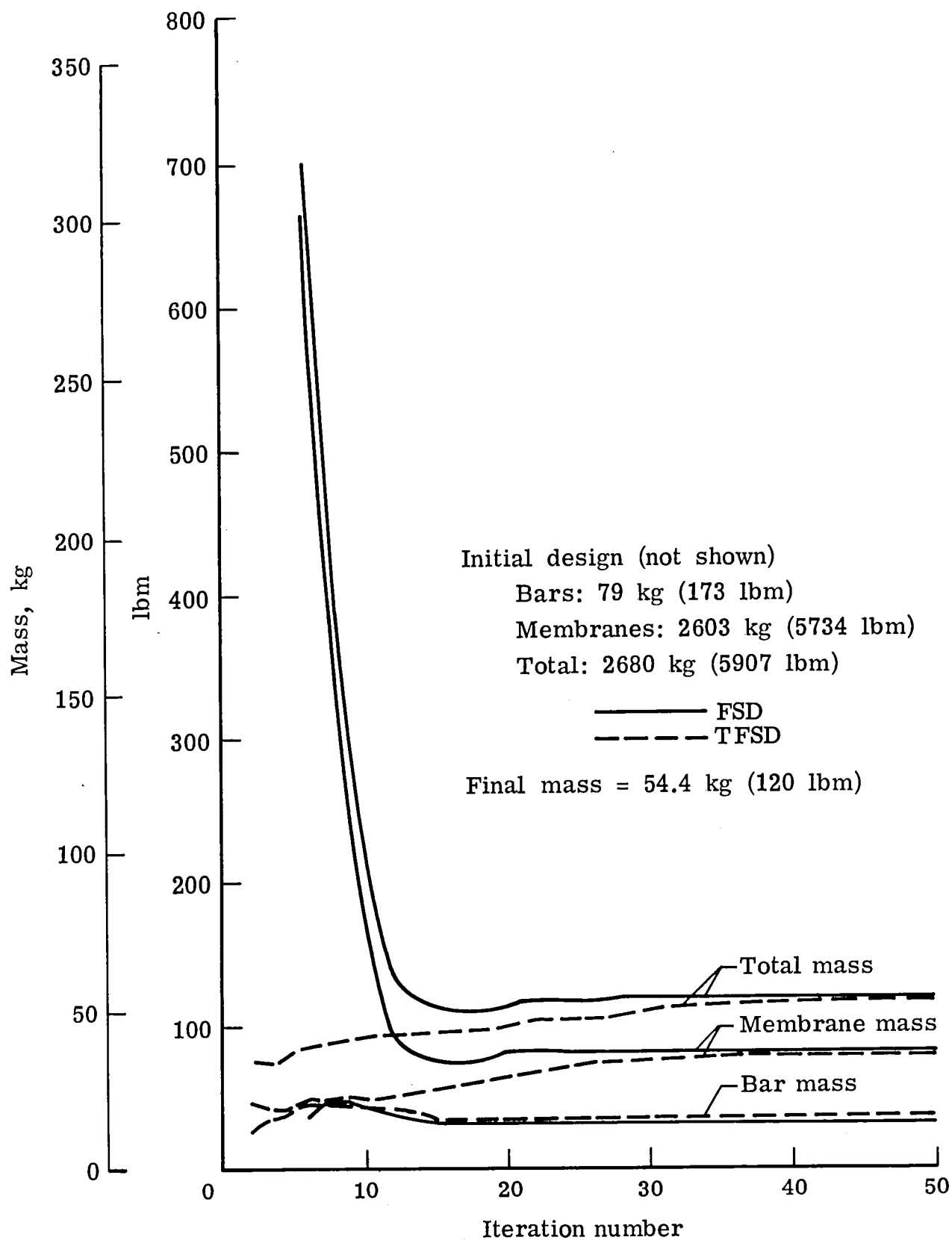
Figure 5.- Convergence of FSD and TFSD for graphite/polyimide box beam. $\Delta T_{upper} = -56$ K (-100° F); $\Delta T_{lower} = 111$ K (200° F).
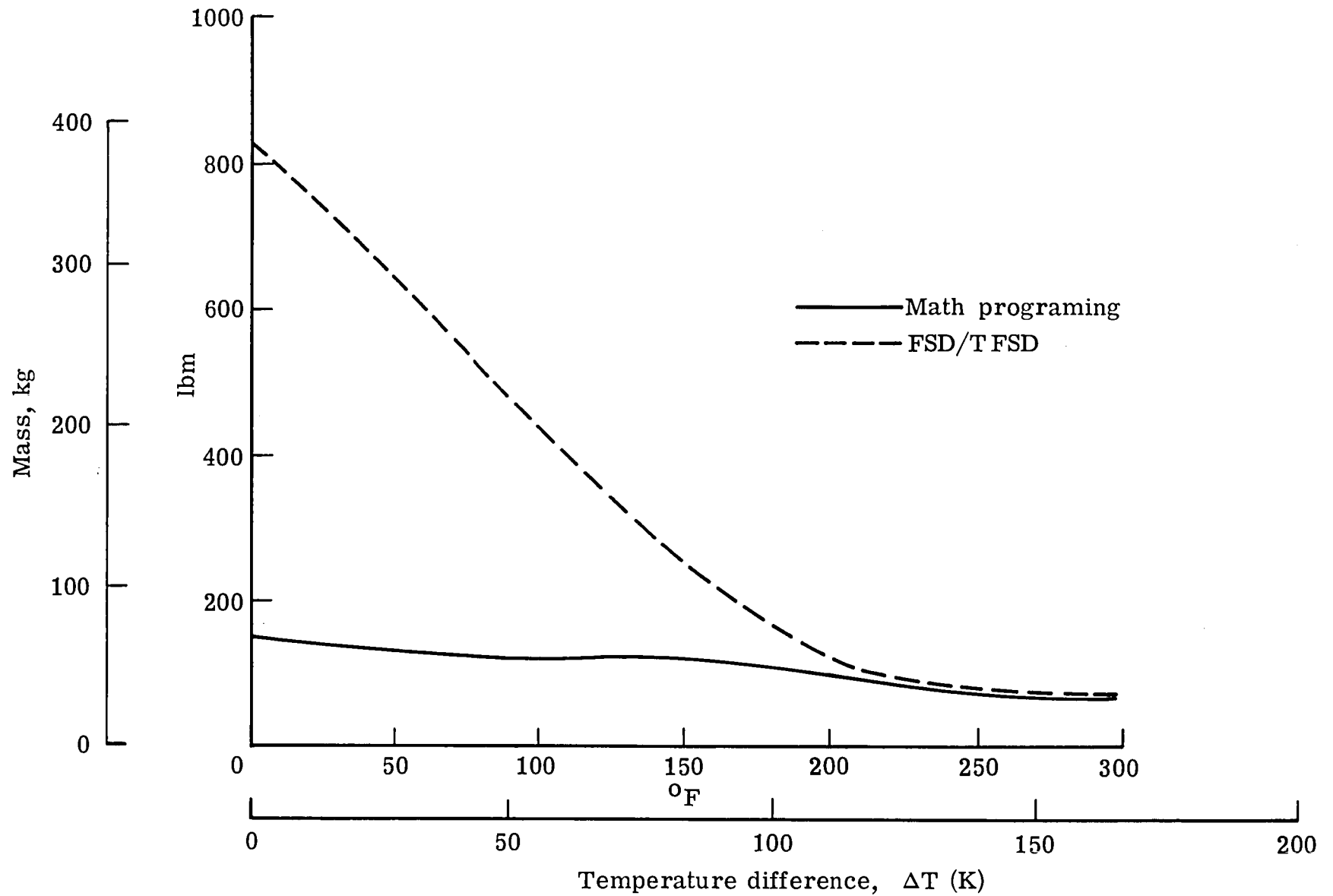
Figure 6.- Effect of temperature loading on agreement between FSD/T FSD
and math programing for minimum mass of graphite/polyimide box beam.

Node numbers
shown for
upper surface
only

Figure 7.- Finite element model of delta wing (top view).
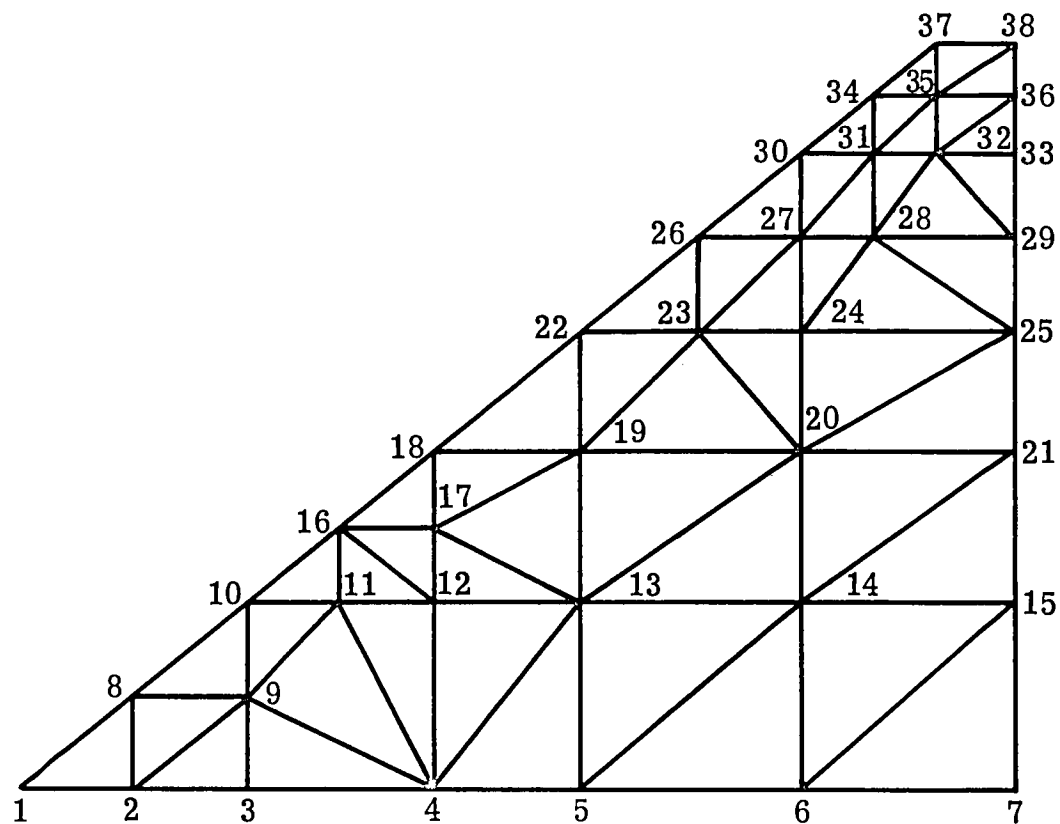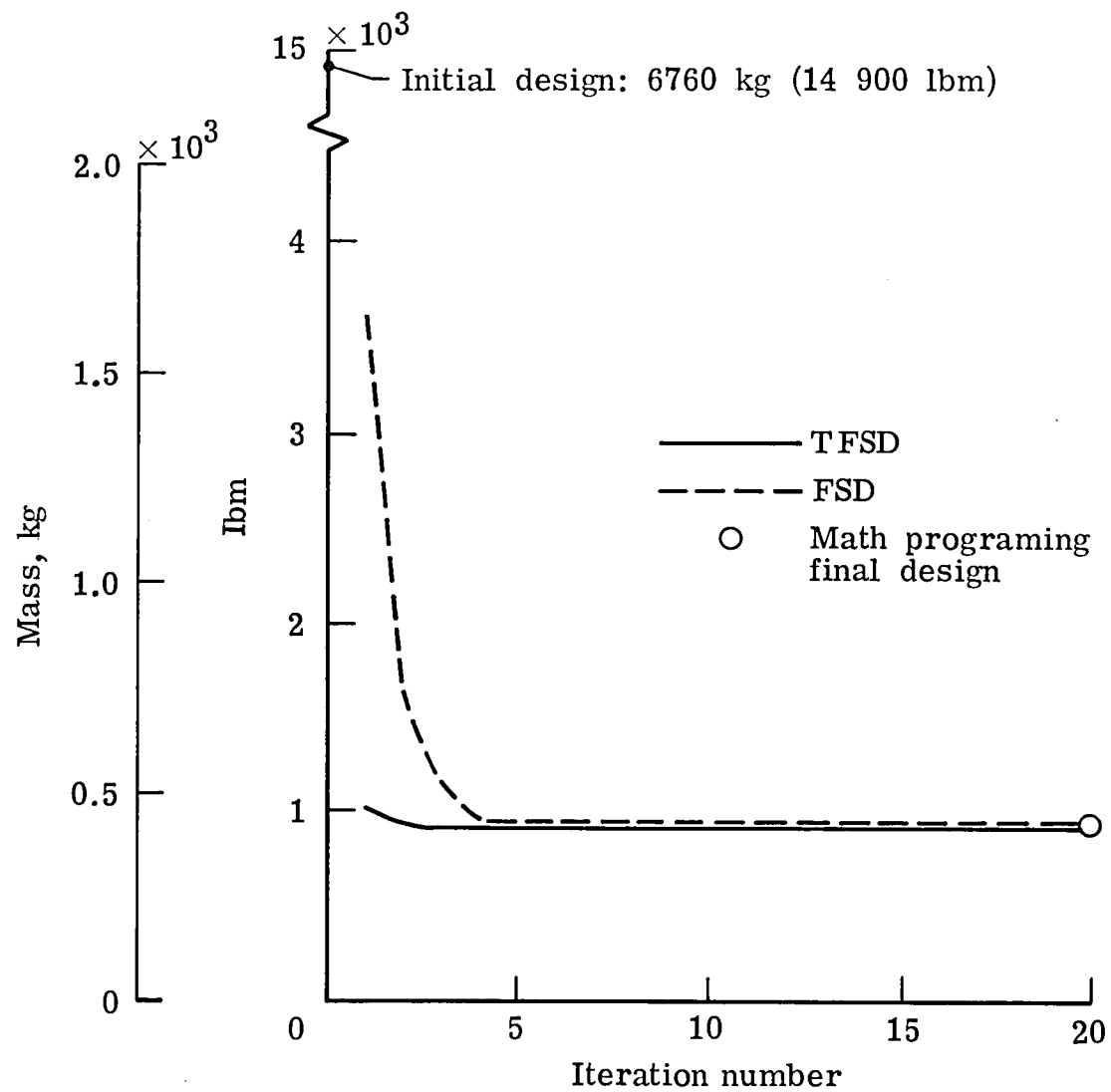
Figure 8.- Convergence of TFSD and FSD for a heated delta wing (skin sizing only).
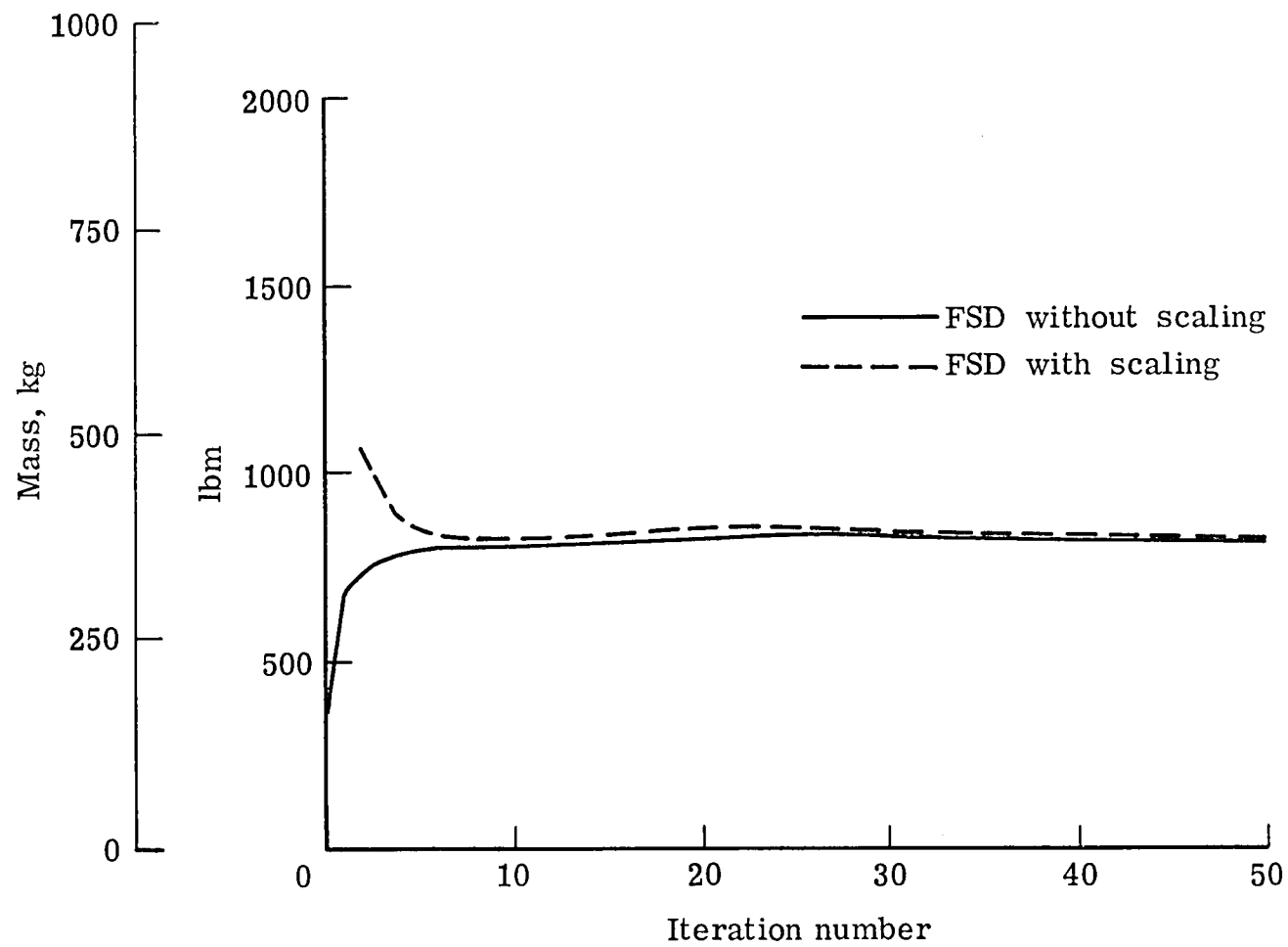
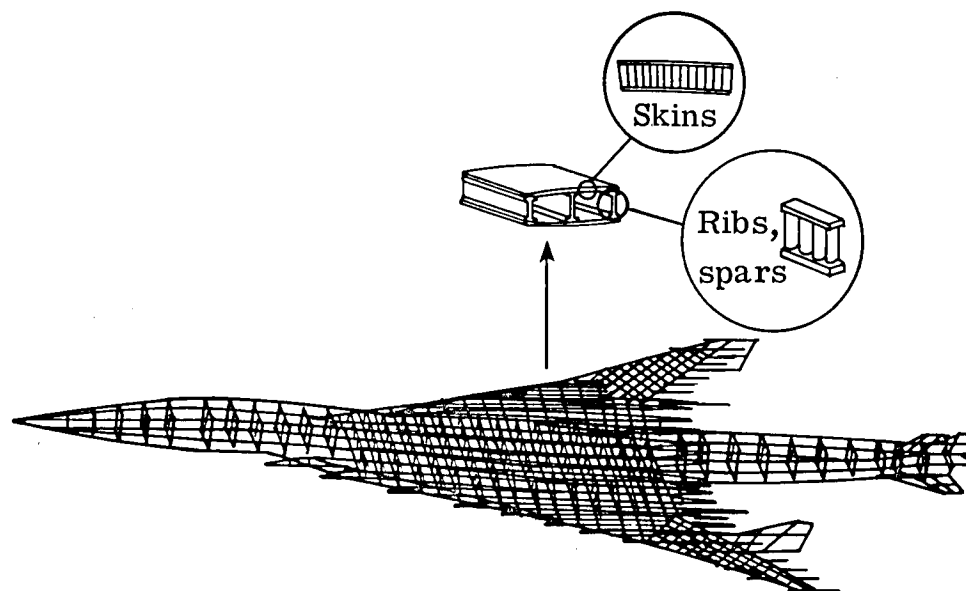Figure 9.- Convergence of FSD with and without scaling for unheated delta wing.

Figure 10.- Finite-element model of arrow wing with details of the wing construction.
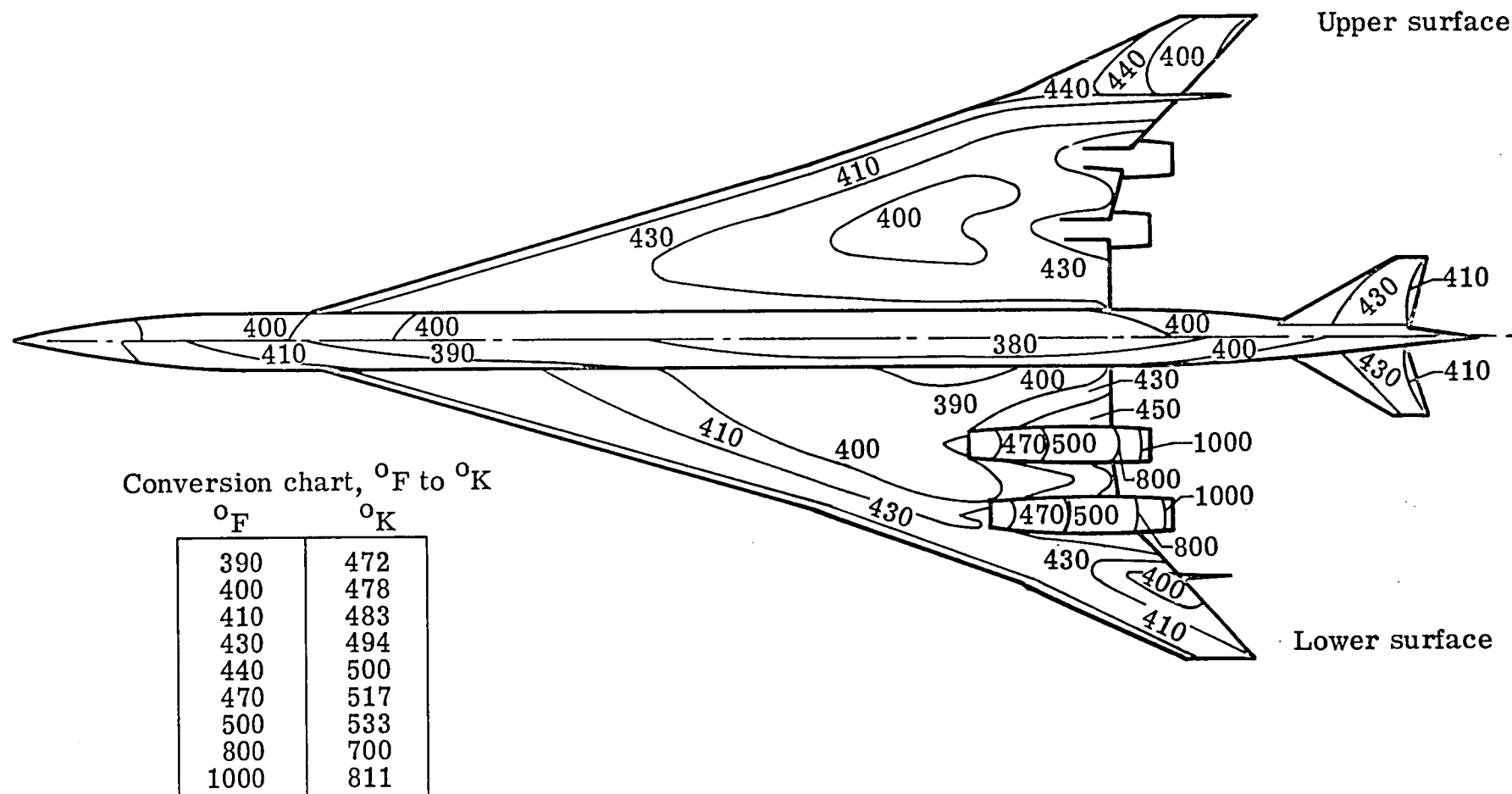
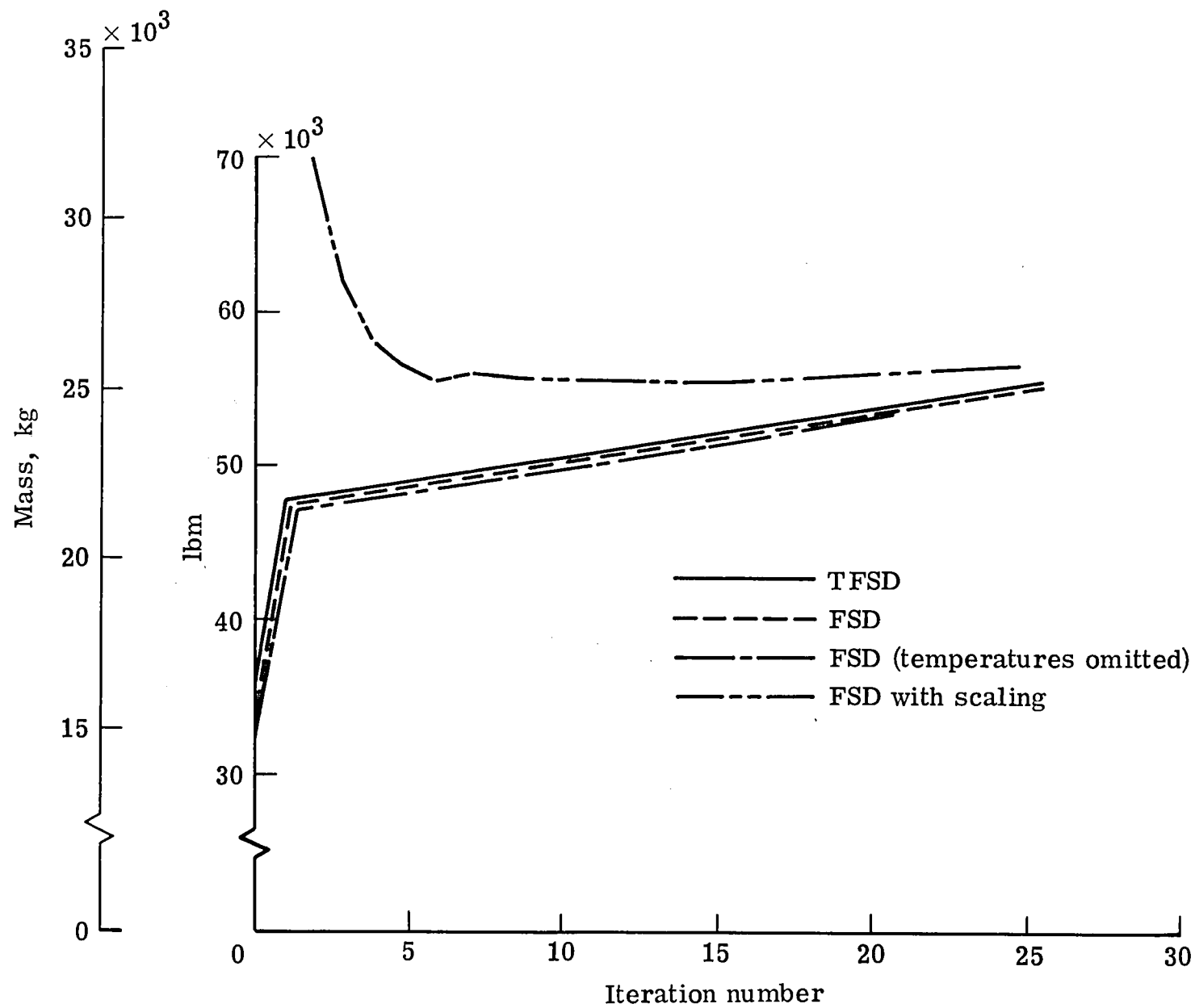Figure 11.- Arrow wing temperature distribution (° F).

Figure 12.- Convergence of TFSD and FSD for arrow wing model. Temperatures based on Mach 2.7 cruise.
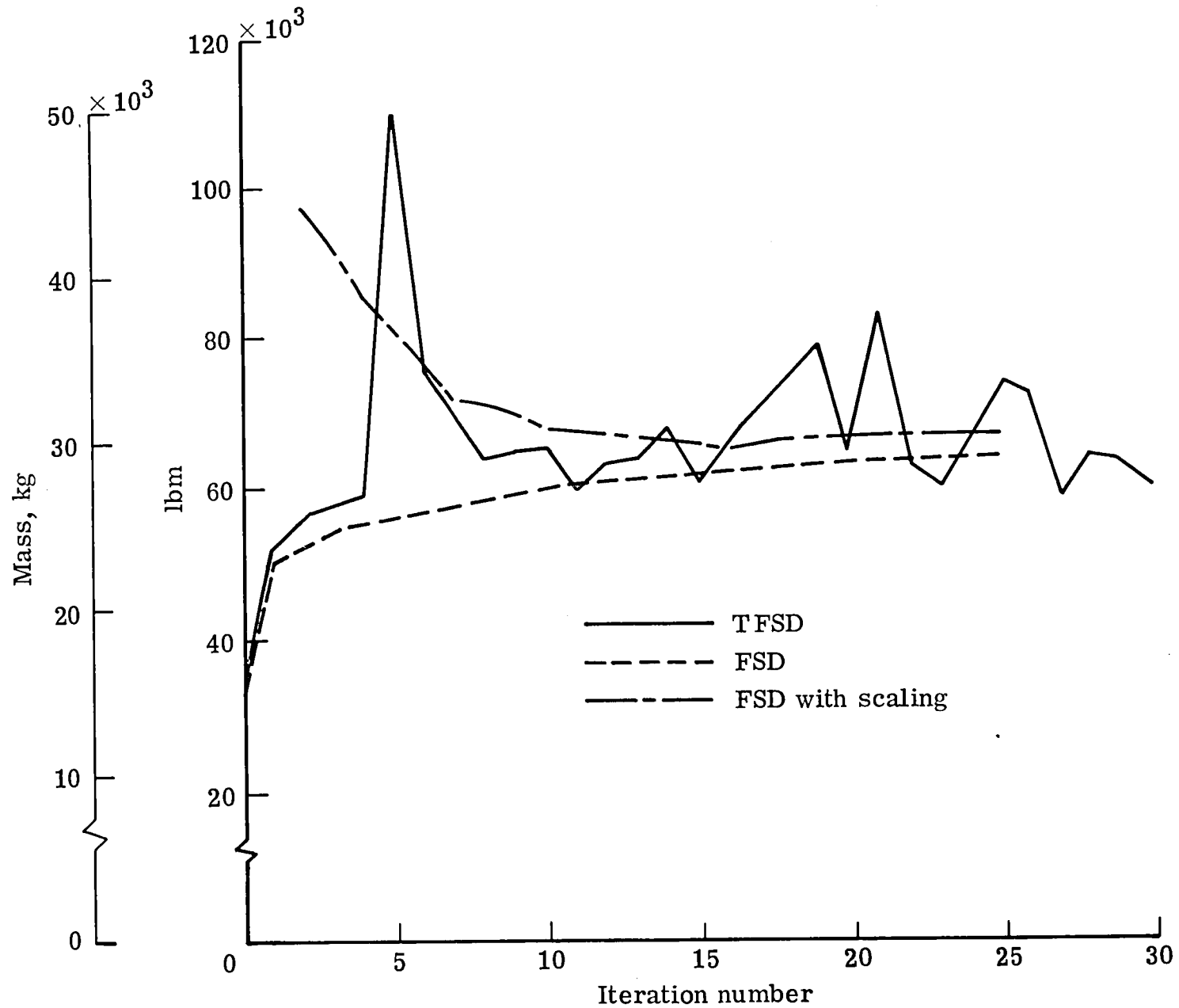
Figure 13.- Convergence behavior of TFSD and FSD for arrow wing model. Temperatures in engine regions = 811 K (1000°F). Remaining temperatures based on Mach 2.7 cruise.

33

1. Report No. NASA TM-81842	2. Government Accession No.	3. Recipient's Catalog No.
4. Title and Subtitle Application of Fully Stressed Design Procedures to Redundant and Non-Isotropic Structures		5. Report Date July 1980
		6. Performing Organization Code
7. Author(s) Howard M. Adelman, Raphael T. Haftka[1] and Uri Tsach[2]		8. Performing Organization Report No.
		10. Work Unit No. 506-53-53
9. Performing Organization Name and Address NASA Langley Research Center Hampton, VA. 23665		
		11. Contract or Grant No.
		13. Type of Report and Period Covered Technical Memorandum
12. Sponsoring Agency Name and Address National Aeronautics and Space Administration Washington, DC 20546		
		14. Sponsoring Agency Code

15. Supplementary Notes

[1]Department of Mechanics and Mechanical and Aerospace Engineering, Illinois Institute of Technology
[2]Department of Mechanical Engineering, Massachusetts Institute of Technology

16. Abstract

This paper discusses an evaluation of fully stressed design procedures for sizing highly redundant structures including structures made of composite materials. The evaluation is carried out by sizing three structures: a simple box beam of either composite or metal construction; a low aspect ratio titanium wing; and a titanium arrow wing for a conceptual supersonic cruise aircraft. All three structures are sized by ordinary fully-stressed design (FSD) and thermal fully stressed design (TFSD) for combined mechanical and thermal loads. Where possible, designs are checked by applying rigorous mathematical programing techniques to the structures. It is found that FSD and TFSD produce optimum designs for the metal box beam, but produce highly non-optimum designs for the composite box beam. Results from the delta wing and arrow wing indicate that FSD and TFSD exhibit slow convergence for highly redundant metal structures. Further, TFSD exhibits slow oscillatory convergence behavior for the arrow wing for very high temperatures. In all cases where FSD and TFSD perform poorly either in obtaining non-optimum designs or in converging slowly, the assumptions on which the algorithms are based are grossly violated. The use of scaling, however, is found to be very effective in obtaining fast convergence and efficiently produces safe designs even for those cases when FSD and TFSD alone are ineffective.

17. Key Words (Suggested by Author(s)) Fully Stressed Design, thermal stress Composite Structures, optimization Wing Structure	18. Distribution Statement Unclassified - Unlimited Subject Category 39		
19. Security Classif. (of this report) Unclassified	20. Security Classif. (of this page) Unclassified	21. No. of Pages 33	22. Price* A03